KLOE note n.149
July 1995

An Automated Facility for Stringing the Large KLOE Chamber

G. Bencivenni
For the KLOE Collaboration

ABSTRACT

The design of the large drift chamber for KLOE reflects the experiment's aim of studying $\mathcal{CP}$-violation in K decays. The KLOE drift chamber is cylindrical in shape, with a radius of about 2 m and a length of about 3.3 m, providing adequate path for K_{L} decays. Spherical end walls which hold the tension of about 50,000 wires, have to be transparent to photons from pion decays. Alternating stereo wires only, with constant radial displacement at the center, will provide a uniform filling with approximately square cells of $3\times3\,\mathrm{cm}^2$. The chamber point resolution is specified to be about 200 microns. It is a monumental task to string this huge number of aluminum and tungsten wires correctly without error and with timeliness, and does not seem to be feasible manually. For this purpose we have designed and are constructing an automated stringing facility which brings the wire from each hole from one end-plate to the appropriate corresponding one in the other end-plate, threading a spindle, and crimping it, all automatically. A full description of this whole set up is in this paper.

THE KLOE COLLABORATION

A. Aloisio,[e] A. Andryakov,[b] A. Antonelli,[b] M. Antonelli,[b] F. Anulli,[b] C. Avanzini,[h] D. Babusci,[b] C. Bacci,[j] R. Baldini-Ferroli,[b] G. Barbiellini,[m] M. Barone,[h] K. Barth,[c] V. Baturin,[e] H. Beker,[h] G. Bellettini,[g] G. Bencivenni,[b] S. Bertolucci,[b] C. Bini,[h] C. Bloise,[b] V. Bocci,[i] F. Bossi,[b] P. Branchini,[k] L. Bucci,[h] A. Calcaterra,[b] R. Caloi,[h] P. Campana,[b] G. Capon,[b] M. Carboni,[b] G. Cataldi,[d] S. Cavaliere,[e] F. Ceradini,[j] L. Cerrito,[i] M. Cerù,[h] F. Cervelli,[g] F. Cevenini,[e] G. Chiefari,[e] M. Cordelli,[b] P. Creti,[d] A. Doria,[e] F. Donno,[b] R. De Sangro,[b] P. De Simone,[b] G. De Zorzi,[h] D. Della Volpe,[e] A. Denig,[c] G. Di Cosimo,[h] A. Di Domenico,[h] E. Drago,[e] V. Elia,[d] O. Erriquez,[a] A. Farilla,[a] G. Felici,[b] A. Ferrari,[g] M. L. Ferrer,[b] G. Finocchiaro,[b] D. Fiore,[e] P. Franzini,[h,f] A. Gaddi,[b] C. Gatto,[e] P. Gauzzi,[h] E. Gero,[b] S. Giovanella,[h] V. Golovatyuk,[d] E. Gorini,[d] F. Grancagnolo,[d] W. Grandegger,[b] E. Graziani,[k] U. v. Hagel,[c] M. Imhof,[c] M. Incagli,[g] C. Joram,[c] L. Keeble,[b] W. Kim,[l] W. Kluge,[c] F. Lacava,[h] G. Lanfranchi,[h] P. Laurelli,[b] J. Lee-Franzini,[b,l] G. Margutti,[h] A. Martini,[b] A. Martinis,[m] M. M. Massai,[g] R. Messi,[i] L. Merola,[e] S. Miscetti,[b] S. Moccia,[b] F. Murtas,[b] M. Napolitano,[e] E. Pace,[b] G. F. Palamà,[d] M. Panareo,[d] L. Paoluzi,[i] E. Pasqualucci,[i] M. Passaseo,[h] A. Passeri,[k] V. Patera,[b] F. Pelucchi,[b] E. Petrolo,[h] M. Piccolo,[b] M. Pollack,[l] L. Pontecorvo,[h] M. Primavera,[d] F. Ruggieri,[a] R. D. Schamberger,[l] C. Schwick,[b] A. Sciubba,[h] F. Scuri,[m] A. Smilzo,[e] S. Spagnolo,[d] E. Spiriti,[k] C. Stanescu,[k] L. Tortora,[k] P. M. Tuts,[f] E. Valente,[h] P. Valente,[b] G. Venanzoni,[g] S. Veneziano,[h] S. Weseler,[c] R. Wieser,[c] S. Wölfle,[b] Y. G. Xie,[n] A. Zallo,[b] C. D. Zhang,[n] J. Q. Zhang.[n]

[a] Dipartimento di Fisica dell'Università e Sezione INFN, Bari
[b] Laboratori Nazionali di Frascati dell'INFN, Frascati
[c] Institut für Experimentelle Kernphysik, Universität Karlsruhe
[d] Dipartimento di Fisica dell'Università e Sezione INFN, Lecce
[e] Dipartimento di Scienze Fisiche dell'Università e Sezione INFN, Napoli
[f] Physics Department, Columbia University, New York
[g] Dipartimento di Fisica dell'Università e Sezione INFN, Pisa
[h] Dipartimento di Fisica dell'Università e Sezione INFN, Roma I
[i] Dipartimento di Fisica dell'Università e Sezione INFN, Roma II
[j] Dipartimento di Fisica dell'Università di Roma III e Sezione INFN, Roma I
[k] Istituto Superiore di Sanità and Sezione INFN, ISS, Roma.
[l] Physics Department, State University of New York at Stony Brook
[m] Dipartimento di Fisica dell'Università e Sezione INFN, Trieste/Udine
[n] Institute of High Energy Physics of Academica Sinica, Beijing, China, joined in 1995

1. Introduction

The main physics objective of the KLOE experiment at DAΦNE, the Frascati ϕ-factory, is the measurement of the ε'/ε parameter down to a precision of 10^{-4} [1,2].

The apparatus is composed by a hermetic electromagnetic calorimeter for the K neutral decay detection and by a large drift chamber for the K charged decay reconstruction [3]. The entire apparatus is immersed in a 0.6 T axial magnetic field.

The design of the drift chamber is driven by the following considerations:

- the main decay path of K_{L} decays at rest is $\sim 3.5\,\mathrm{m}$, thus the K_{L} decay vertices are spread over a large volume of the chamber;
- the momentum of charged pions from K decay is practically uniformly distributed in the range $150 \div 270\,\mathrm{MeV}/c$;
- photons from π^0 decay, in the energy range $50 \div 300\,\mathrm{MeV}$, should encounter traversing the chamber as less material as possible before reaching the calorimeter.

All the above considerations reflect in the choice of the chamber dimensions and mechanical structure, cell shape and size, gas mixture and wire material. Low Z materials (carbon fibre) for the chamber mechanical structure, helium based gas mixture and aluminum alloys for wires (at least for field and guard wires, the most numerous component) are required in order to reduce as much as possibile photon conversion, multiple scattering and K_{S} regeneration probabilities.

In addition one has to maximize the fiducial volume and achieve a high and well controlled efficiency for $K_{\mathrm{L}} \to \pi^+\pi^-$ decays. All these requirements lead to a chamber design with very thin walls and a huge number of wires ($\sim$ 50,000), therefore requiring a careful study of the wires characteristics and feed-through design as well as a wiring strategy based on a semi-automatic approach.

The outline of this paper is as follows: the mechanical design of the drift chamber and the cell design are discussed in section 2; the wire choice in section 3; the feed-through design and test in section 4; the chamber wiring strategy and the stringing machine design are discussed in section 5.

2. Mechanical Structure and Cell Design

2.1 Mechanical Structure

In order to minimize the photon conversion before the electromagnetic calorimeter and reduce the multiple scattering and the energy losses of charged particles entering the chamber all the walls of the chamber structure must be as thin as possibile. Consequently stiff materials, especially for the end-plates, must be employed to maintain the mechanical deformations (due to the global wire load) at an acceptable level.

The KLOE drift chamber, shown in fig. 1, is a cylinder of $\sim 2\,\mathrm{m}$ radius and $\sim 3.7\,\mathrm{m}$ long. The two end-plates are spherical (flat end-plates would give unacceptable deformations), with a radius of curvature of $\sim 9.7\,\mathrm{m}$, and kept apart by twelve struts attached to the outer flange. The end plates are made of a $8\,\mathrm{mm}$ ($\sim 0.03 X_0$) high stiffness isotropic carbon fibre-resin composite (Young modulus $\approx 8{,}000\ \mathrm{kg/mm^2}$). Twelve panels, honeycomb structured, provide the needed torsional rigidity to the chamber and, together with the very thin ($\sim 0.7\,\mathrm{mm}$) carbon fibre inner cylinder, the required gas tightness.

Finite element calculations and tests on small scale prototypes [4] showed that, for a global wire load of $\approx 4{,}000\,\mathrm{kg}$, the axial deformation of the end-plate is of the order of $2 \div 3\,\mathrm{mm}$. In order to further reduce this deformation, which affects the wire sagitta (hence the wire position) uniformity, an additional stiffening ring properly attached to the outer flange has been included in the chamber design [5]. Calculations have shown that this solution allows the end-plate deflexion to be kept below $0.5\,\mathrm{mm}$.

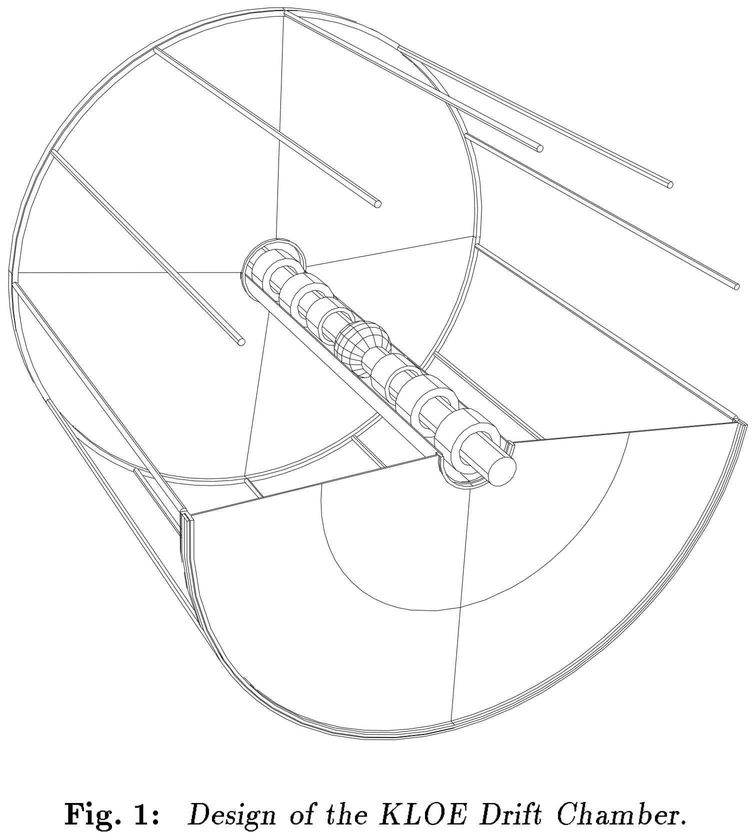

Fig. 1: *Design of the KLOE Drift Chamber.*

2.2 Cell Design

The uniform distribution of K_L decay vertices and secondary tracks in the chamber volume requires a constant size drift cell. The uniform filling of the sensitive volume is obtained by means of square cells arranged in circular layers with alternating stereo angles. All stereo layers move radially inward with a constant maximum displacement δ=1.5 cm at z=0 (chamber center). The stereo angle increases as $\sqrt{R_i}$, (R_i being the chamber radius), from ~ 60 mrad up to ~ 150 mrad.

The choice of 3×3 cm^2 square cells, with a ratio of field to sense wire of 3:1, minimizing the multiple scattering and the global wire load, allows to maintain a proper time-space relation over most of the cell along the z-axis. Simulation studies have shown that the single track losses and the overall loss for full $K_L\to\pi^+\pi^-$ reconstruction obtained with a 3×3 cm^2 cell size are only slightly larger than those obtained with a 2×2 cm^2 cell [6]. Therefore, taking into account the large difference in total number of wires and electronic channels the 3×3 cm^2 cell represents an acceptable compromise. Nevertheless, an inner region of 12 layers of 2×2 cm^2 cells has been implemented in order to maximize the extent of the fiducial volume by allowing the reconstruction of short backward going tracks from K_L decays.

In tab. 1 the global number of sense, field and guard wires are shown.

Configuration	N. layers	N. sense	N. field	N. guard	total N. wires
2×2 cm^2	12	1404	4212	168	5784
3×3 cm^2	46	11178	34410	768	46356
total	58	12582	38622	936	52140

Tab. 1: *KLOE Wire Configuration.*

3. Wire Choice

3.1 Sense Wire

For sense wire we decided to use 25 μm diameter gold plated tungsten wire. This is a standard choice [8,9] for drift chambers if a small wire diameter is required. The diameter choice is correlated to the required gas gain of $\sim 10^5$. Tests performed on small scale prototypes with the KLOE cell configuration have proven that a gas gain greater than 10^5 is achieved at about 2,000 V high voltage power supply. The mechanical characteristics of the tungsten wire adopted for the KLOE drift chamber are shown in tab. 2.

diameter (μm)	25.
Au plating thick. (μm)	0.25
ovality (%)	≤ 2
weight tolerance (%)	≤ 1.5
elastic limit (gr)	100.
ultimate tensile (gr)	140.

Tab. 2: *Tungsten Wire Characteristics.*

For good gain uniformity, to prevent sparking and for high reliability, the wire must meet very stringent requirements.

The impact of the sense wires on the chamber transparency is not negligible. The presence of the tungsten wires (uniformly spread inside the chamber volume) does reduce the radiation length of the $90\%\mathrm{He}-10\% i\mathrm{C_4H_{10}}$ gas mixture ($\sim 1300\,\mathrm{m}$), down to $\sim 1{,}000\,\mathrm{m}$.

The main drawback of tungsten is that soldering is not a reliable method for fixing the wire. The problem, as discussed later, can be overcome by using crimping techniques.

3.2 Field and guard wire

For field and guard wires, aluminum is the natural choice for the following reasons:

- aluminum has the longest radiation length of any practical material. In fact, in terms of multiple scattering contribution, copper beryllium wire would degrade the momentum resolution of a factor of $(15 \div 20)\%$ with respect to aluminum wire;
- due to their low density, aluminum wires require 30% less tension for a given gravitational sag than the more conventional Cu-Be choice, considerably lessening the global load on the end-plates.

The solution adopted for the KLOE chamber is a 5056 aluminum alloy $\sim 80\,\mu$m diameter wire, similar to that one used in CLEO II chamber [10].

The field wire diameter is set by the necessity of avoiding spontaneous electron emission on cathodes and gas amplification near the field wire surface [11]. In tab. 3 the main characteristics of the two different 5056- aluminum wire configuration (with and without surface plating) considered for the KLOE drift chamber are shown.

	Al-5056(no plating)	Al-5056+Ni flash+ Ag(1 μm)
diameter (μm)	82.4	83.2
density (gr/cm^3)	2.64	2.89
X_0 (cm)	8.9	7.6
elastic limit (gr)	$\sim$ 350	$\sim$ 350
ultimate tensile (gr)	$\sim$ 410	$\sim$ 410

Tab. 3: *5056 Aluminum Wire Characteristics.*

Gold plated aluminum wire has been rejected to avoid the addition of too heavy material inside the chamber volume ($\sim 1\,\mu$m thick gold plating shortens the wire equivalent radiation length by $\sim 50\%$ respect to bare aluminum wire).

Because aluminum wire has not been frequently used in drift chambers, we considered necessary to perform long-term mechanical behaviour study as well as doing ageing test. To study the long-term creeping of the aluminum wire, several samples (~ 1500 mm long) were suspended under a constant tension of 100 gr and their length variations monitored by means of a theodolite for a period of ~ 6 months. A couple of Cu-Be ($100\,\mu$m diameter) wires have been used as reference to monitor possibile global movements of the entire set-up. Local temperature has also been monitored to allow thermal length change subtraction. The result of the measurement (at constant tension), in agreement with data given in literature [12] for similar aluminum alloy, is compatible with a wire tension drop smaller than 5%.

Ageing as well as cathodic breakdown study on helium based gas mixtures has been performed by V'avra [13]. For some gas mixture configurations and for too small diameter (and not perfect wire surface quality) field wires ageing and sparking problems can occur because ionization electrons tend to be hot even at modest electric fields if the amount of quenching gas used in the mixture is too small.

For this reasons we performed [7] ageing tests with different field to sense wire ratios ($\mathcal{R}_{\rm fs}$ = 2 and 3), using a $90\%{\rm He}-10\%i{\rm C_4H_{10}}$ gas mixture. The radiation source used for the test was an X-ray tube with tungsten target emitting 10 keV X-ray plus a bremsstrahlung continuum up to 25 keV energy. As summarized in tab. 4 negligible gas gain drop has been observed in both wire configurations considered, after an integrated charge of $2 \div 3$ mC/cm.

	Al-5056(no plating)	Al-5056+Ni flash+Ag(1 μm)
int. charge (mC/cm)	3.1	2.5
$\Delta G/G$ (%)	~ 0	~ 5

Tab. 4: *Aluminum Wire Ageing.*

Defining 1 KLOE operation year as $\sim 100\,\mu$C/cm (the Bhabha dose accumulated on one cm of the innermost wire of the chamber during one year of running at the maximum machine luminosity), the above values of integrated charge correspond to about $20 \div 30$ years of KLOE operation.

4. Feed-Through Design

The system used to hold the wires is one of the most critical components of the drift chamber. Taking into account the large number of wires involved ($\sim 50{,}000$) the scheme to fix them should satisfy very stringent requirements:

- high mechanical and electrical reliability over the entire chamber lifetime (≥ 5 years);
- high positioning precision ($\leq 30\,\mu$m);
- fast realization of the wire fixation in series production.

All these requirements are easily fulfilled by the crimping pin method, performed by clamping the pin on one side by means of a special designed crimping jaw. Special care must be taken on the pin material choice:

- good electrical conductivity;
- good cutting and machining properties;
- high ductility;
- ease of gold plating,

and should clearly match as far as possibile the field and sense wire material chosen. After several tests we chose Cu-OFHC pins.

Fig. 2 shows the complete arrangement of crimping pin and plastic insulating bushing adopted for tungsten and (tempered) 5056-aluminum alloy wires. Metal pins are realized by precision machining of mini-tubes obtained from drawn tubes. Internal pin holes are 100 and 150 μm diameter respectively for sense and field wires. The insulating bushing, made of DELRIN [14], is coupled to the metal pin by means of an injection moulding technique, ensuring good gas tightness.

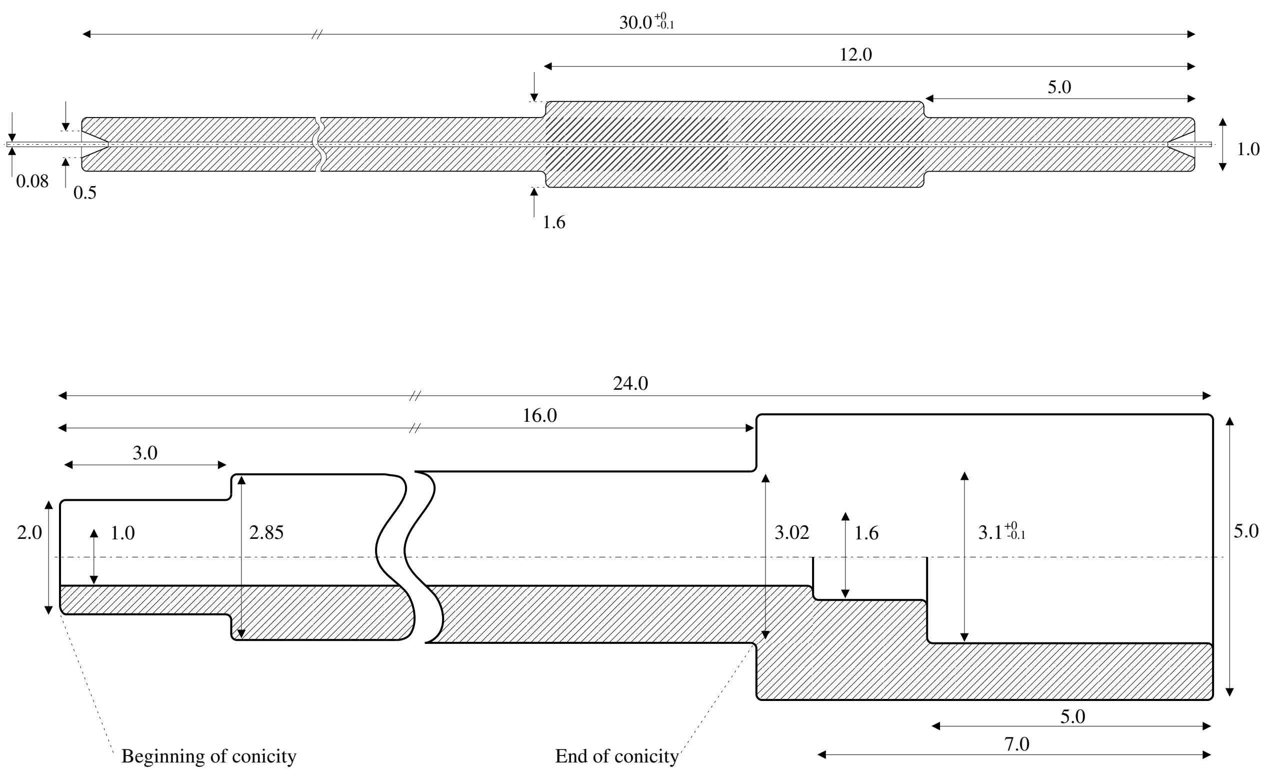

Fig. 2: *Crimping pin and insulating bushing arrangement for KLOE drift chamber.*

Crimping can be made via either manual or pneumatic clamping jaws. Flat or cylindric shaped jaws can be adopted. Different crimping sizes (defined as the thickness of the pin after crimping) can be achieved by changing the jaws or tuning the value of the pressure supply if a manual or a pneumatic tool is used respectively as crimping device.

The pin material choice as well as the crimping pin design are the result of a systematic study on the wire/pin coupling. The crimping method, successfully used on several drift chambers [9,10], should allow us to solidly held the wire along several millimeters, without deformations nor damages. Wire shape deformations around the crimping area imply severe damages of the wire resulting on wire weakening and possible wire breaking. Our studies have shown that if the pin material is harder than the wire itself, the latter will lose its round shape and will be damaged.

Fig. 3 shows a cross section of the wire/pin coupling on the crimped area for different wires and pin material choices at a fixed value of $\sim 0.7\,\mathrm{mm}$ crimping size. It is seen that, for the non-tempered 5056-aluminum wire, the aluminum pin is better than the copper one, while if tempered aluminum wire is used, the copper pin is the best choice.

For tungsten wire, copper pins ensure a reliable coupling.

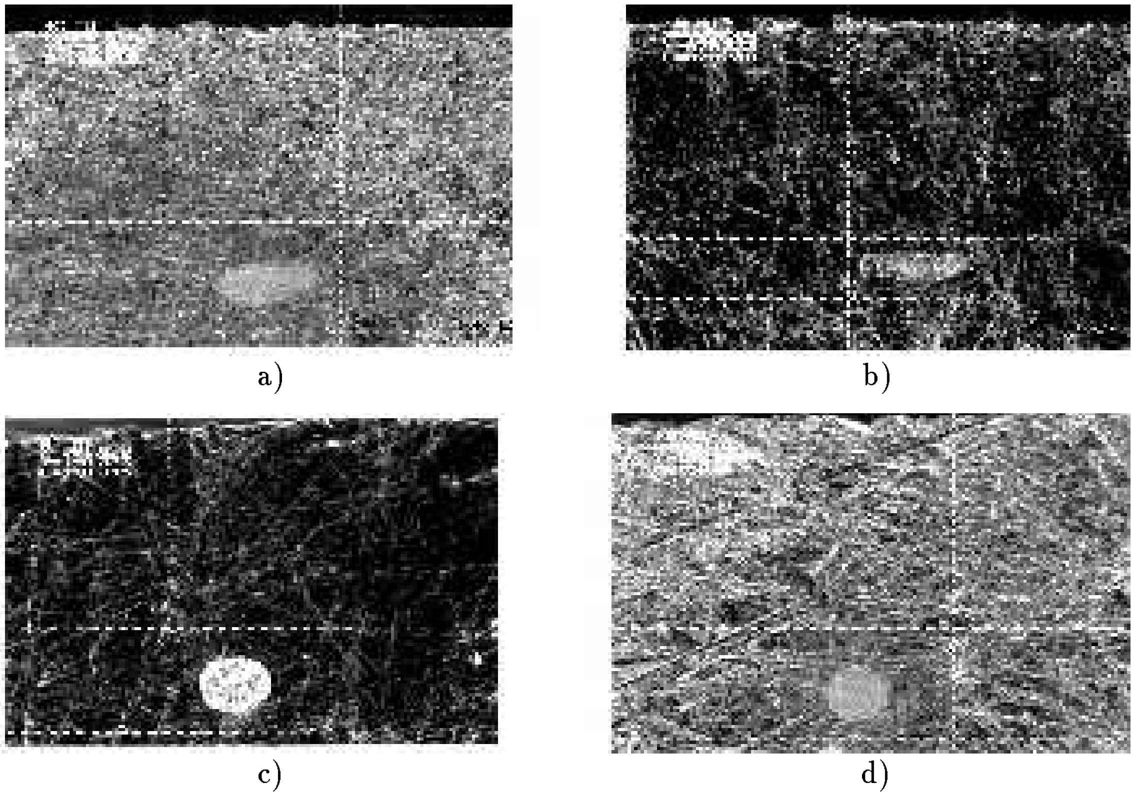

Fig. 3: *Cross section of the wire/pin coupling in the crimped area for copper pin and Al 5056 wire: a) non-tempered; b) non-tempered+Au (1.3* μm*); c) tempered+Au (0.5* μm*); d) tempered+Au (1.0* μm*).*

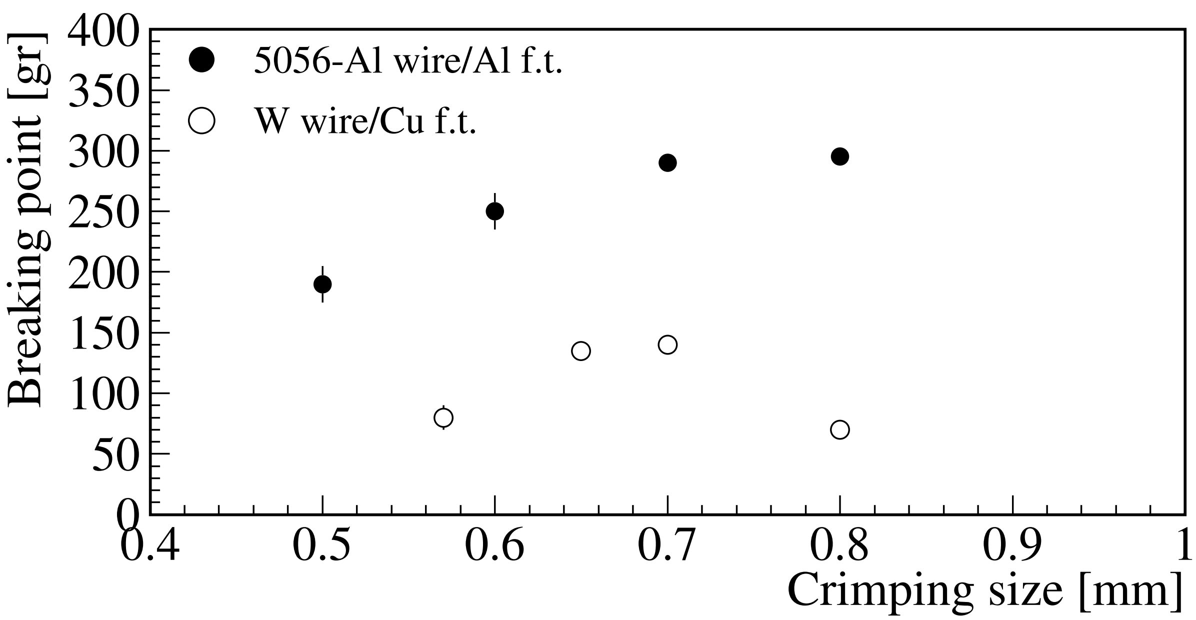

Fig. 4: *Wire breaking point as a function of the crimping size for the aluminum and the tungsten wires, respectively.*

The above considerations, based on the optical survey of the wire/pin coupling in the crimping zone, are widely confirmed by the results obtained by studying the mechanical resistance of the wire/pin coupling.

The results, shown in fig. 4, show that for crimping ≤ 0.65 mm both wires (tungsten and aluminum) break earlier than their nominal value; for crimping size ≥ 0.75 mm the wires slip through the pin (generally at tension values smaller than their ultimate tensile). A crimping size of ~ 0.7 mm the wire/pin coupling is the optimal choice, in fact wires break at values of tension very similar to their ultimate tensile. Wire/pin coupling tests for the tempered silver plated aluminum wire have been performed at a fixed crimping size of 0.7 mm (fig. 5).

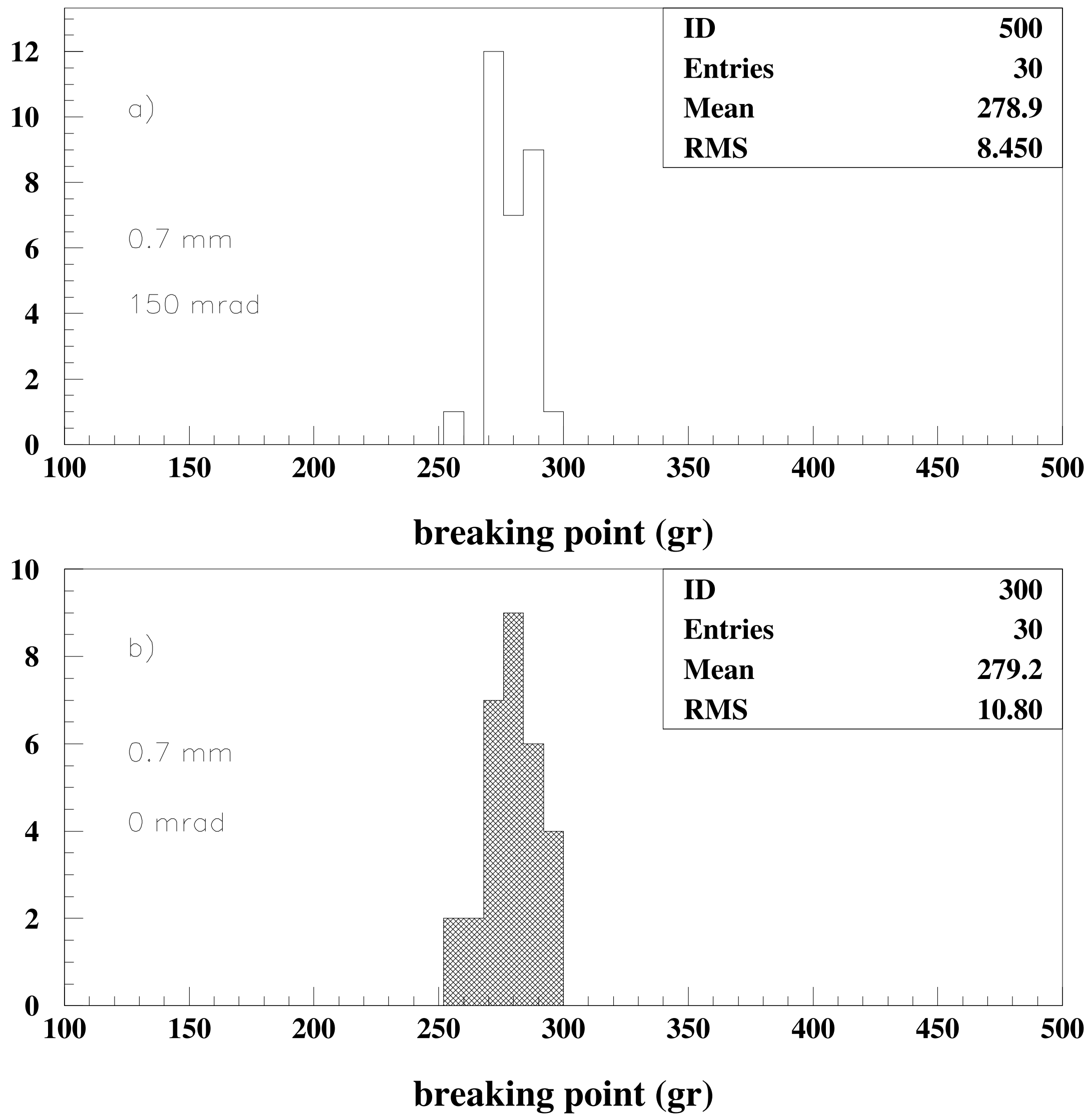

Fig. 5: *Wire breaking point distribution for the tempered silver plated 5056 aluminum wire.*

4.1 Feed-Through tolerances

Besides the hole position accuracy ($\sim 50\,\mu$m) on the end-plates, several feed-through design parameters affect the wire location precision. The measured tolerances on the different feed-through components are shown in tab. 5. The global contribution of feed-through tolerances on the wire location accuracy is $\sim 30\ \mu$m.

pin/bushing concentricity (μm)	22.
pin-hole concentricity (μm)	13.
feed through location accuracy in end-plate hole (μm)	15.
crimping position accuracy (μm)	8.

Tab. 5: *Feed-through tolerances.*

The feed-through location accuracy in the end-plate holes essentially depends on the coupling between the bushing and the end-plate hole and then, on the bushing shape. As shown in fig. 6, we found that bushings with a draft of $\sim 13\,\mu$m/mm give the best coupling and positioning accuracy.

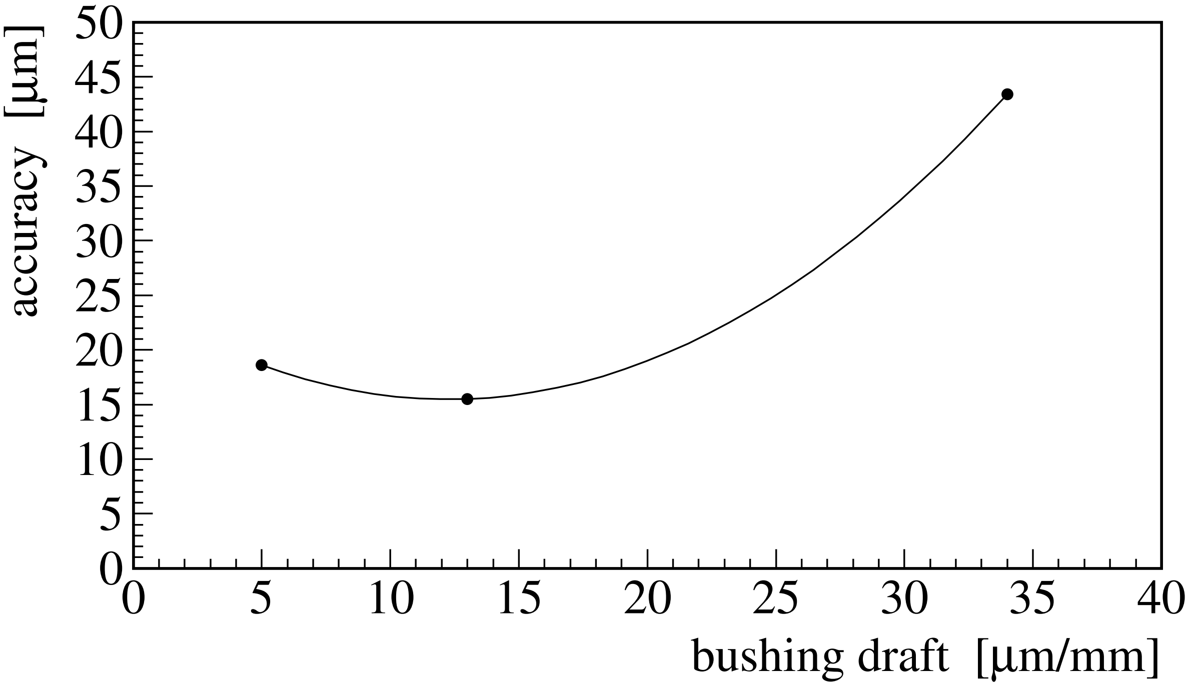

Fig. 6: *Feed-through location accuracy as a function of the bushing draft.*

5. Chamber Wiring Strategy and Stringing Machine

The wiring procedure of the drift chamber must take into account that the chamber end-plates deflect under the wire load, therefore one has to study a stringing strategy to ensure a satisfactory wire sagitta spread (at the level of $\sim 20\,\mu$m) at the end of chamber wiring. As previously discussed the maximum chamber end-plate deformation is $\sim 2 \div 3$ mm. These deflections correspond to a not negligible wire tension drop and wire sag increase.

Considering an average wire length of 3 m, increase in tension drop and wire sag is of the order of 16%/mm and 12%/mm for the aluminum and tungsten wires respectively. Taking into account the wire length difference, due to spherical end-plates (from 2865 mm to 3266 mm for the innermost and outermost wire layers), a very broad wire sagitta distribution is found at the end of chamber stringing (fig. 7).

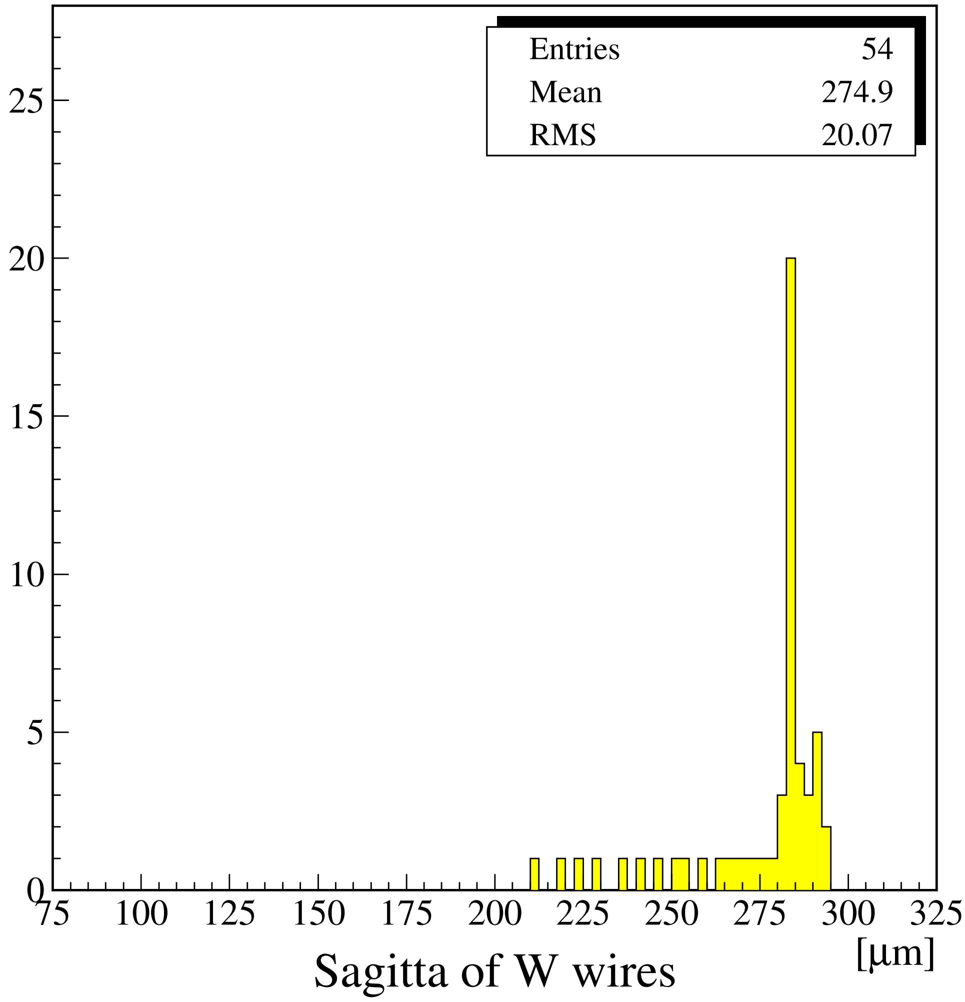

Fig. 7: *Expected wire sag distribution (without end-plate deformation recovery).*

As shown in fig. 8, for a proper choice of the initial wire tension, bigger for the innermost layers and smaller for the outermost ones, a very narrow final sagitta ($\leq 5\,\mu$m rms) distribution will be obtained.

Considering that the stiffening ring, pulling radially the end-plate, makes for an appreciable reduction of the end-plate deformations down to 0.5 mm, a further improvement on the final wire sagitta uniformity is expected.

The KLOE drift chamber will be wired in a "class 1000" clean room, both humidity ($50\pm1\%$) and temperature ($20\pm1^\circ$C) controlled.

Besides the large stringing area, the clean room will house a separate small room used for the acceptance sampling test of wires and feed-throughs. The wire surface quality test and the wire diameter check will be performed by means of a microscope coupled to a video-micrometer. A computer controlled wire stretching device will inspect the mechanical characteristics of the wires and the wire/feed-through coupling. All the information will be stored on disk.

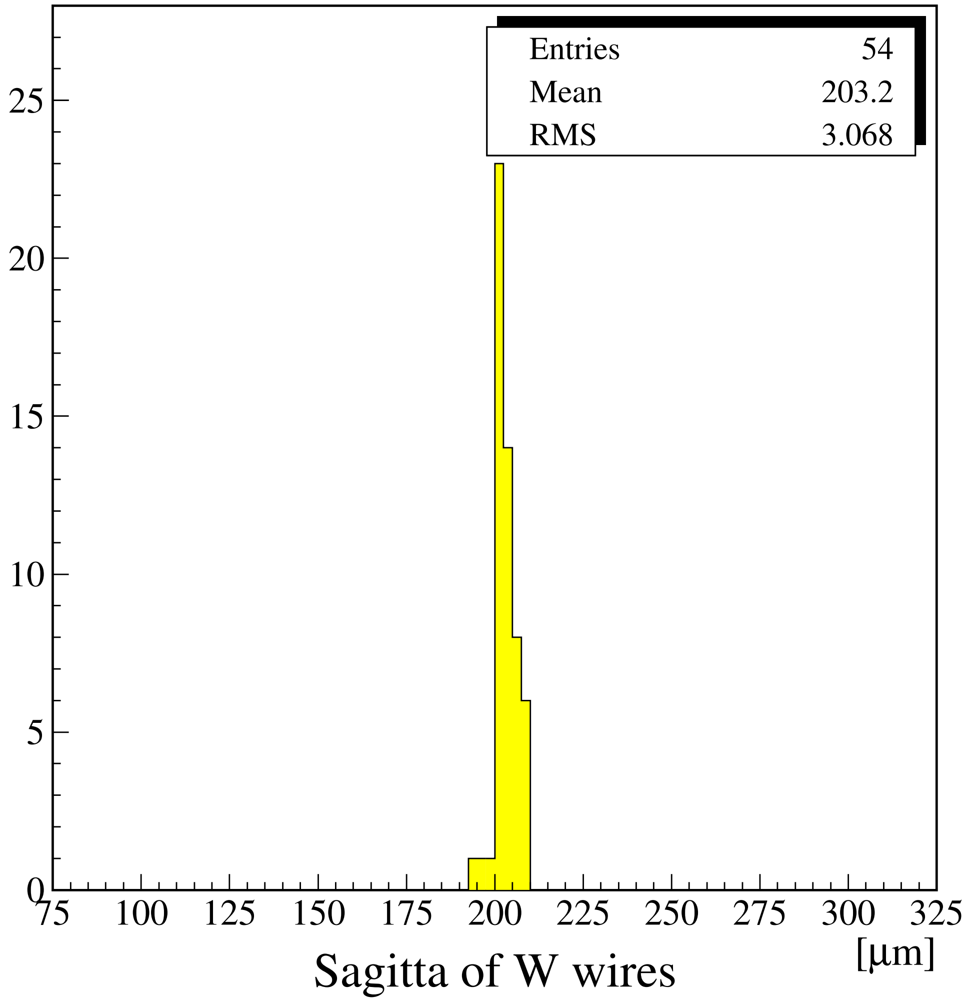

Fig. 8: *Expected wire sag distribution (with end-plate deformation recovery).*

The drift chamber will be strung horizontally, by means of a computer controlled machine composed by three main parts (fig. 9):

- a special rig designed to support the chamber end-plates (connected by the twelve struts not – shown in the picture) and the other parts of the stringing machine, and allowing the chamber to rotate during stringing;

- two crimping and tensioning stations located externally at the end-plate sides;
- an automated arm moving inside the chamber catching and bringing the wire from one end-plate to the other.

The main rig has been designed in order to ensure the required chamber torsional rigidity. End-plates are fixed by means of flanges to a central rotation tube. The coupling between the flanges and the tube is performed by means of linear bearing allowing the end-plates to freely move axially, as is necessary to take into account the end-plate deformation under wire load. The rotation is done by coupling the tube to a speed reduced step motor. The tube is fixed to the main rig by means of circular bearing. The rotation mechanics provides a chamber positioning accuracy of about $0.2 \div 0.3\,\mathrm{mm}$ at the end-plate edge ($R \sim 2\,\mathrm{m}$).

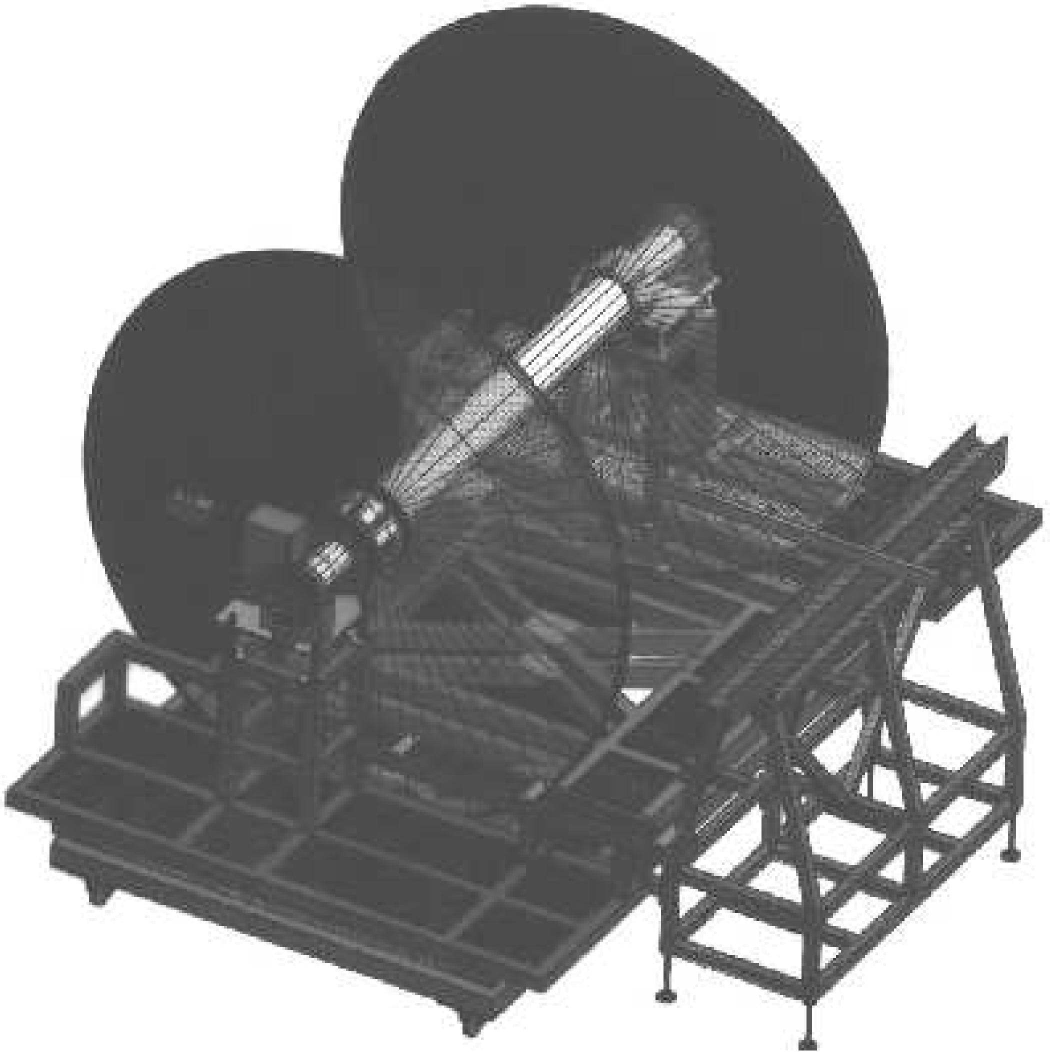

Fig. 9: *The Stringing Machine design.*

A fine chamber positioning monitoring, at a level of $0.05\,\mathrm{mm}$ at $R \sim 2\,\mathrm{m}$, is achieved by means of a high resolution incremental encoder coupled to the rotation system. This precision level is required for a good positioning of the crimping and tensioning device mounted on the external stringing stations (to avoid pin breaking due to possibile misalignment between crimping tool and pin).

Both external stringing stations include an XYZ axis system moved by step motors and coupled to incremental encoders for position monitoring. One of the two stations (the wire sending one) is equipped with a double wire spooling system (for aluminum and tungsten wire) a torque gauge for wire tensioning and a pneumatic crimping tool. The second station (the wire receiving one) is equipped only with a crimping tool.

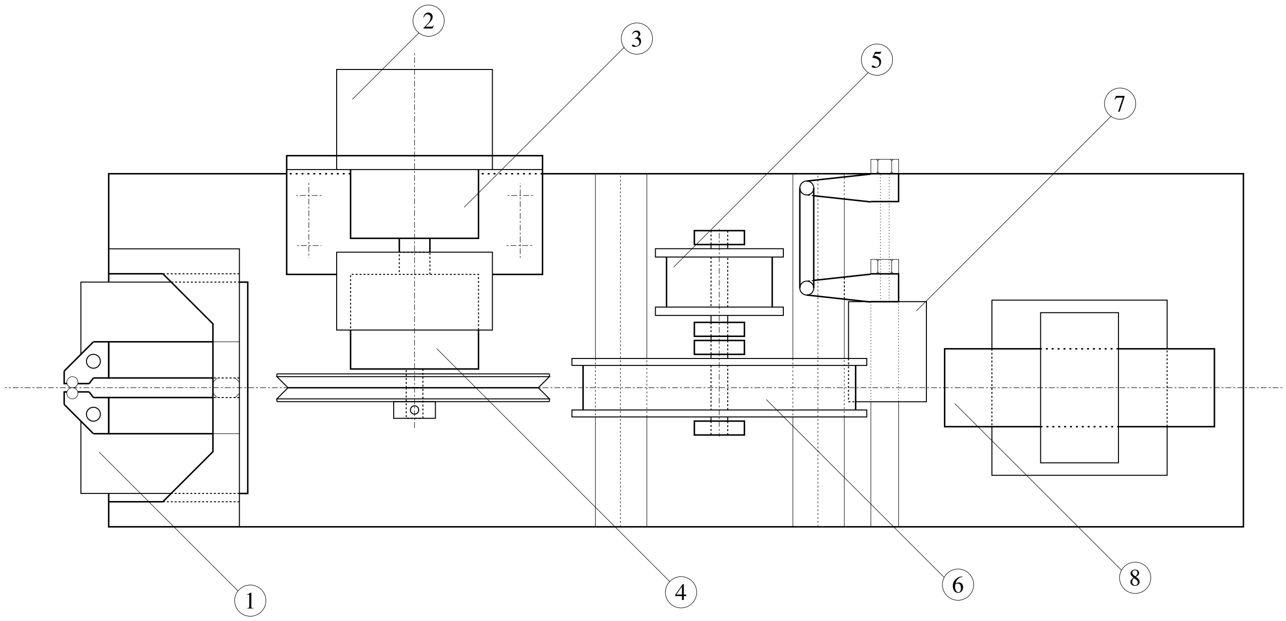

Fig. 10: *The pneumatic jaw design. 1: pneumatic crimping jaw; 2: step motor; 3: epicyclic reduction gear; 4: torque-meter; 5: tungsten wire spool; 6: aluminum wire spool; 7: pneumatic cylinder; 8: telecamera.*

The crimping jaw, shown in fig. 10, is similar to the one successfully used for the stringing of the $\sim$ 2,500 wires of the full length chamber prototype [3,15]. Wires are carried from one end-plate to the other one by an XYZ automated system, equipped with two identical wire handling tools designed to catch and hold the wire along the transportation, without damaging it.

Once the wire is inserted into the inlet cone of the wire handling tool, it is pulled by two rotating precision cylinders, see fig. 11. When the wire has arrived to the beginning of the outlet cone the cylinder rotation is stopped by a grounding sensor and the automated arm starts to move toward the corresponding hole on the second end-plate. At this time, the cylinder motor starts again pushing the wire through the hole. The operator, picking the wire up stops the cylinder motor, inserts the wire through the pin and starts the computer controlled crimping operation. The wire stringing operation will be completed on the other end-plate side by pulling the excess wire slack, tensioning the wire with the proper tension and crimping the feed-through.

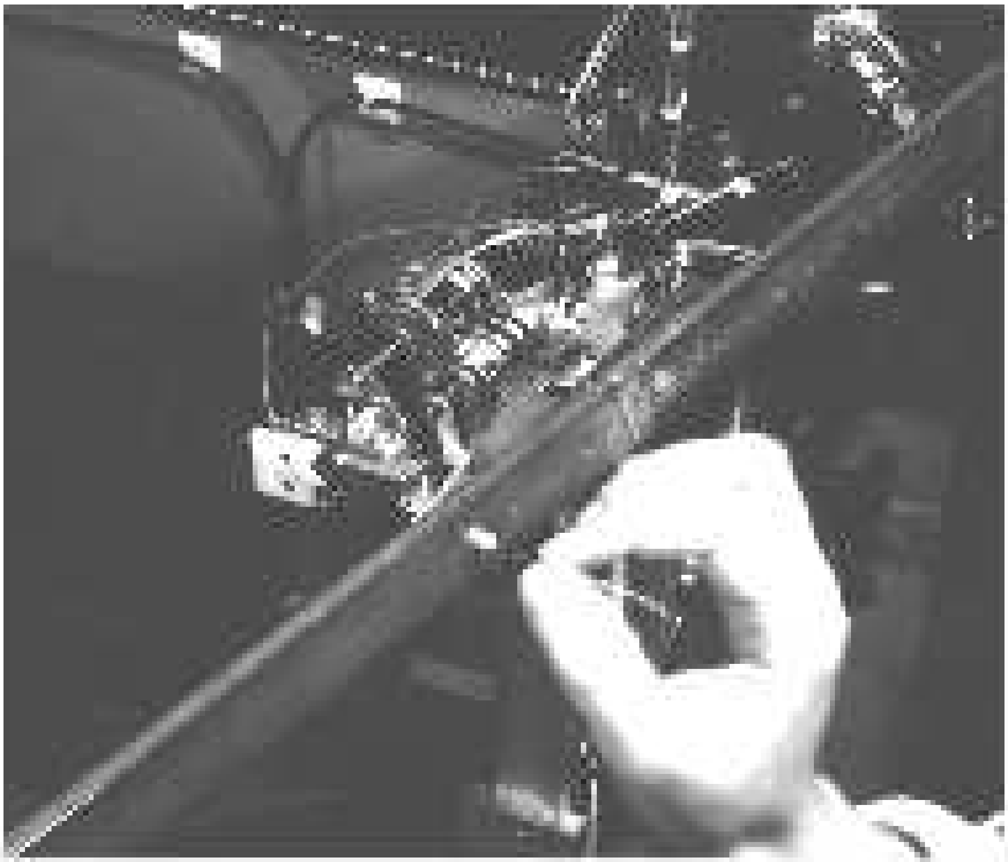

Fig. 11: *Prototype of the wire handling tool during a test phase.*

6. Summary

We discussed the mechanical features and the construction choices, concerning wires, feed-through and stringing procedure for the KLOE drift chamber. For chamber stringing we are going to adopt a semi automatic approach which, ensuring a very clean operation, will allow us to complete the chamber wiring in about 9 months.

ACKNOWLEDGEMENTS

We would like to acknowledge F. Bronzini and A. Pelosi for the design of the support and rotation system of the chamber; R. Assiro and G. Fiore for the design and realization of the automated crimping and tensioning stations; G. Catitti and E. Iacuessa for the design and construction of the automated arm for the wire handling; U. Denni and M.A. Frani for the realization of the automation of the stringing machine. We also acknowledge Dr. R. De Salvo, Dr. D. Peterson and Dr. E. Rosso for their useful suggestions.

REFERENCES

1. The KLOE Collaboration, *A General Purpose Detector for* DAΦNE, LNF-019/1992.
2. The KLOE Collaboration, *The KLOE Detector, Technical Proposal*, LNF-002/1993.
3. The KLOE Collaboration, *The KLOE Central Central Drift Chamber, Addendum to the Technical Proposal*, LNF-028/1994.
4. A. Gaddi and S. Moccia, *Mechanical Structure of the KLOE Drift Chamber*, KLOE note n. 55 (Apr. 1993).
5. G. Petrucci, *A suggestion for minimizing the end plates deformation of cylindrical wire chambers*, KLOE note n. 53 (Mar. 1993).
6. A. Andryakov, P. De Simone, V. Patera, M. Pollack, *MC Study of Drift Chamber performance*, KLOE note n. 105 (Mar. 1994).
7. G. Bencivenni, L. Bucci, R. de Sangro, G. Finocchiaro, P. Valente, *Ageing Test of the KLOE Drift Chamber Wires*, KLOE note n. 143 (Apr. 1995).
8. R.D. Heuer and A. Wagner, *NIM* **A265**, 11 (1988).
9. B. Foster *et al.*, *NIM* **A338**, 254 (1994).
10. D.G. Cassel *et al.*, *NIM* **A252**, 325 (1986).
11. P. Giubellino *et al.*, *NIM* **A252**, 528 (1986); R. Bouclier *et al.*, *CERN-PPE*, 95-36 (1995); Proc. of the Workshop on Radiation Damage to Wire Chambers, *LBL*, Jan. 16-17 1986 (LBL-21170).
12. L. Lazzarino and E.Manfredi, *Meccanica dei Materiali*, E.T.S. Editrice, Pisa (1988).
13. J. Va'vra, *NIM* **A324**, 113 (1993).
14. DELRIN is a trademark of the Dupont Corporation.
15. The KLOE Collaboration, *Full Scale Prototype of the KLOE Drift Chamber*, KLOE note n. 145 (Apr. 1995).

TABLE CAPTIONS

1. KLOE Wire Configuration.
2. Tungsten Wire Characteristics.
3. 5056 Aluminum Wire Characteristics.
4. Aluminum Wire Ageing.
5. Feed-through tolerances.

FIGURE CAPTIONS

1. Design of the KLOE Drift Chamber.
2. Crimping pin and insulating bushing arrangement for KLOE drift chamber.
3. Cross section of the wire/pin coupling in the crimped area for different wire and pin materials.
4. Wire breaking point as a function of the crimping size for a) the aluminum wire and b) the tungsten one.

5. Wire breaking point distribution for the tempered silver plated 5056-aluminum wire.
6. Feed-through location accuracy as a function of the bushing draft.
7. Expected wire sag distribution (without end-plate deformation recovery).
8. Expected wire sag distribution (with end-plate deformation recovery).
9. The Stringing Machine design.
10. The pneumatic jaw design.
11. Prototype of the wire handling tool during a test phase.